



## **Assessment of Personnel Accessibility in the X-1 Facility**

**H.Y. Khater, M.E. Sawan, R.R. Peterson**

**October 2000**

**UWFDM-1135**

Presented at the 14th Topical Meeting on the Technology of Fusion Energy,  
October 15–19, 2000, Park City UT

***FUSION TECHNOLOGY INSTITUTE***

***UNIVERSITY OF WISCONSIN***

***MADISON WISCONSIN***

### **DISCLAIMER**

This report was prepared as an account of work sponsored by an agency of the United States Government. Neither the United States Government, nor any agency thereof, nor any of their employees, makes any warranty, express or implied, or assumes any legal liability or responsibility for the accuracy, completeness, or usefulness of any information, apparatus, product, or process disclosed, or represents that its use would not infringe privately owned rights. Reference herein to any specific commercial product, process, or service by trade name, trademark, manufacturer, or otherwise, does not necessarily constitute or imply its endorsement, recommendation, or favoring by the United States Government or any agency thereof. The views and opinions of authors expressed herein do not necessarily state or reflect those of the United States Government or any agency thereof.

# ASSESSMENT OF PERSONNEL ACCESSIBILITY IN THE X-1 FACILITY

H. Y. Khater, M. E. Sawan and R. R. Peterson  
Fusion Technology Institute  
University of Wisconsin  
1500 Engineering Dr., Madison, WI 53706  
(608) 263-2167

## ABSTRACT

Hands-on maintenance activities outside the X-1 aluminum chamber may be allowed within a few hours following radiation (photoneutron) shots. Dose rates outside the chamber following moderate yield (200 MJ) shots are four orders of magnitude higher than those following radiation shots. In the mean time, dose rates following high yield (1000 MJ) shots are a factor of five higher than those following moderate yield shots. Hands-on maintenance is allowed outside the chamber and inside the water tank within 10 and 14 days following moderate and high yield shots, respectively. Access to the area outside the water filled tank is allowed after only a few hours following moderate and high yield shots.

## I. INTRODUCTION

The proposed X-1 experimental facility would use wire array Z-pinchs to produce X-rays for several purposes, including the radiative implosion of Inertial Confinement Fusion (ICF) capsules.<sup>1</sup> In one ICF target concept, approximately 16 MJ of X-rays would be produced by two Z-pinchs, which would be fed to a cylindrical hohlraum from both ends. The hohlraum would be designed to create the proper symmetry for the implosion for ignition of the ICF capsule. Fusion yields of up to 1000 MJ may be achievable with this approach. Another approach would place an ICF fuel capsule inside a pinch, termed a dynamic hohlraum. The blast resulting from the explosion of the capsule would be confined inside a target chamber. The fusion neutrons from yield shots and, to a lesser degree, photoneutrons and ions will activate the experimental chamber. The X-1 experiment chamber will experience a considerably harsher environment than does the National Ignition Facility (NIF) chamber. The challenge of the X-1 design activity is to develop an experiment chamber concept that allows radioactive vapor, molten material and shrapnel to be contained in a way that allows for maintenance and timely operation of the facility.

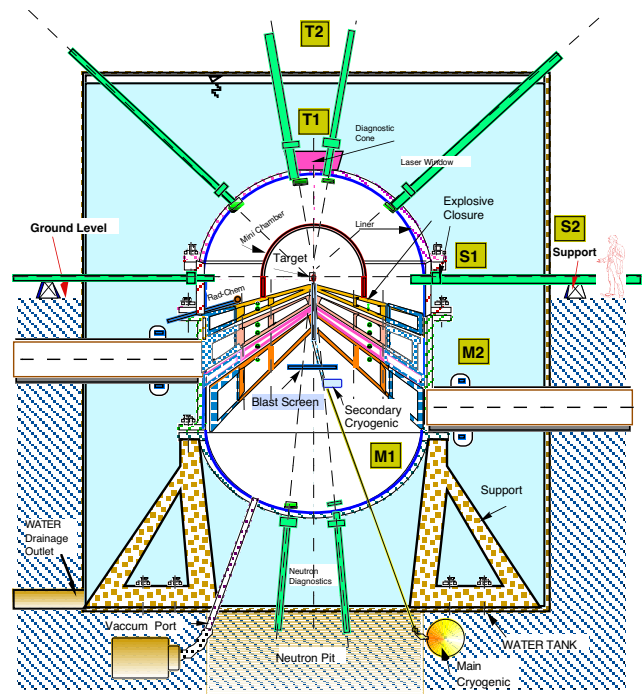


Fig. 1. X-1 Experimental Chamber Design Concept.

The experimental chamber concept is depicted in Fig. 1. The design employs a "defense in depth" strategy. Multiple layers of protection are used to confine the blast generated by the energy contained in the chamber. The first level of protection is the hemispherical mini-chamber made of Kevlar with a graphite inner coating, which is meant to stop the large pieces of magnetic debris, and most of the X-rays and debris ions emitted from the target. The mini-chamber may need replacement after shots with a burning ICF capsule, but it will be designed not to become a debris source itself. The next layer is an aluminum liner that will absorb those X-rays and debris ions that pass through the holes in the mini-chamber. Both the liner and the mini-chamber will experience

significant vaporization and melting. After a shot, the liner can be removed as a unit with the radioactive rubble trapped inside. Fast-closing explosive valves will prevent radioactive debris from leaving the experiment chamber. The liner is attached to the inner surface of an aluminum structural wall designed to carry the impulsive and long-term pressure loading from the blast. Outside of that is a water shield to stop fusion neutrons and gamma rays emitted by radioactive materials.

This experiment chamber concept is flexible with respect to its pulsed power interface. The chamber analyzed in this paper has many long coaxial magnetically insulated transmission lines (MITLs) that converge on the axis of the cylindrical chamber. In order to achieve the goal of allowing for a relatively safe maintenance environment, the blast resulting from the explosion of the ICF fuel capsule is confined inside an aluminum target chamber, submerged in a water tank for shielding purposes. In order to evaluate the radiological hazards associated with performing routine maintenance on the experimental chamber, biological dose rate calculations are performed. The dose rates are calculated at different locations in the vicinity of the chamber and following all types of shots.

## II. CALCULATION APPROACH

Neutronics and shielding calculations are performed using the ONEDANT module of the DANTSYS 3.0 discrete ordinates particle transport code system.<sup>2</sup> A spherical geometry is utilized with the target represented by an isotropic point source in the center. The source emits neutrons and gamma photons with energy spectra determined from target neutronics calculations for a generic target.<sup>3</sup> Figure 2 shows the energy spectrum of neutrons emitted from the target. The neutron flux obtained from the neutron transport calculations is used in the activation calculations. The activation calculations are performed using the computer code DKR-PULSAR<sup>4</sup> with the FENDL-2 activation cross section library.<sup>5</sup> The neutron transmutation data used is in a 46 group structure format. The gamma source data is in 21 group structure format. Using the DKR-PULSAR code allows for appropriate modeling of the pulse sequence in ICF chambers. In a previous analysis of the Laboratory Microfusion Facility,<sup>6</sup> it was shown that assuming an equivalent steady state operation (where the flux level is reduced to conserve fluence) results in underestimating the dose rates at shutdown by several orders of magnitude. The underestimation becomes negligible within a week from shutdown. The large underestimation within a short period of time following shutdown is due to the fact that the activity during this time is dominated by short-lived radionuclides. The activities of short-lived isotopes are usually sensitive to the operational schedule prior to

shutdown due to its buildup during the on time with subsequent decay during the dwell time. On the other hand, the long-term activity is dominated by long-lived radionuclides whose activity is determined by the total neutron fluence regardless of the temporal variation of the flux level.

Biological dose rates are calculated at different locations inside and outside the water tank as a function of time following shots. After initial comparison between chambers made of the Al-5083 and 2 1/4 Cr-1 Mo alloys, the low activation alloy Al-5083 is selected as the preferred chamber material candidate. The calculations are performed for three different types of shots. The first type is radiation shots with a pulsing schedule of 1 shot per day for a total of 240 shots per year. Only photoneutrons are produced during these shots. The photoneutrons are produced as a result of interaction between the Bremsstrahlung radiation and the MITLs. The second type of shots considered is moderate yield shots. These shots produce a fusion yield of 200 MJ and have a pulsing schedule of 2 shots per month for a total of 24 shots per year. The third type of shots considered is the high yield shots. These shots also use a pulsing schedule of 2 shots per month for a total of 24 shots per year with a fusion yield of 1000 MJ.

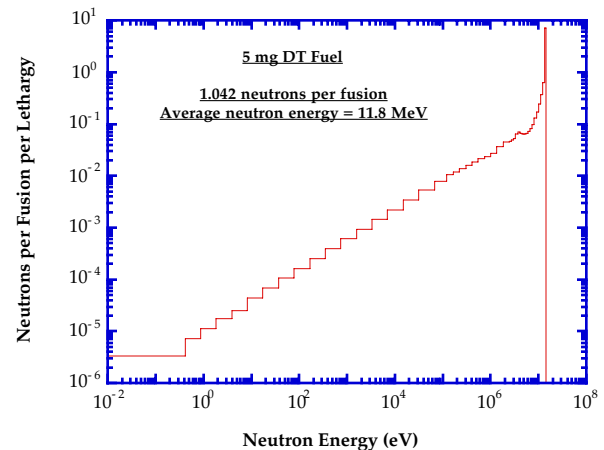


Fig. 2. Energy Spectrum of Neutrons Emitted from the Generic Target

## III. BIOLOGICAL DOSE RATES

The decay gamma source produced by the DKR-PULSAR code is used to calculate the biological dose rate after shots at different locations inside and outside the water tank. The DKR-PULSAR code gives the decay gamma source at different times following shutdown. The adjoint dose field is then determined by performing a gamma adjoint calculation using the DANTSYS code with the flux-to-dose conversion factors representing the source

at the point where the dose is calculated. The decay gamma source and the adjoint dose field are then combined to determine the biological dose rate following shutdown.

### A. Moderate and High Yield Shots

Biological dose rates are calculated at six different locations for different times following shots. These locations are shown in Fig. 1. The two alloys Al-5083 and 2 1/4 Cr-1 Mo steel are considered as chamber material candidates. Figure 3 shows a comparison between the biological dose rates expected outside the chamber and inside the water tank (location "T1") at all times following moderate yield shots for the two alloys. Using the aluminum chamber allows for hands-on maintenance, 10 days following moderate yield shots for the two alloys. On the other hand, using the steel chamber would not allow for hands-on maintenance at all times following shots. Based on these results, the Al-5083 alloy is selected as the preferred chamber material. The remaining results presented in this paper are for a chamber made of the Al-5083 alloy. Finally, in this analysis, the limits for hands-on maintenance were assumed to be at 2.5 mrem/hr. At these low levels, unlimited access is possible. Limited access may also be allowed at higher dose levels.

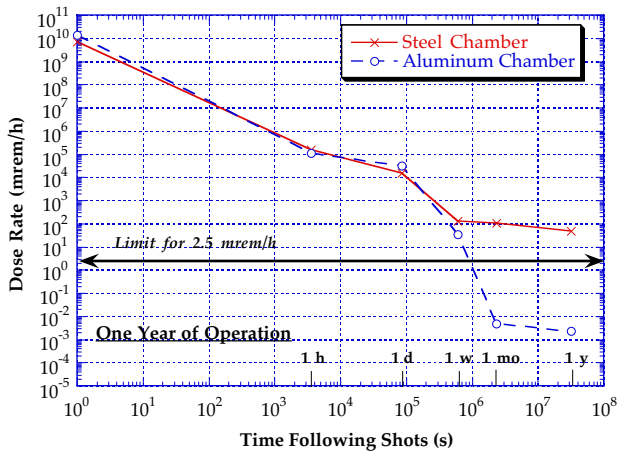


Fig. 3. Biological Dose Rates at Location "T1" Following Moderate Yield Shots.

In the case with aluminum alloy in the chamber wall, the dose rates within the first few minutes following shots are dominated by the decay of  $^{24m}\text{Na}$  ( $T_{1/2} = 20.2$  ms) produced from the  $^{27}\text{Al}(n,\alpha)$  reaction. During the first few hours, the doses are dominated by  $^{24}\text{Na}$  ( $T_{1/2} = 14.96$  hr) produced from the  $^{23}\text{Na}(n,\gamma)$ ,  $^{24}\text{Mg}(n,p)$ , and  $^{27}\text{Al}(n,\alpha)$  reactions and  $^{27}\text{Mg}$  ( $T_{1/2} = 9.45$  min) produced from the  $^{26}\text{Mg}(n,\gamma)$ ,  $^{27}\text{Al}(n,p)$ , and  $^{30}\text{Si}(n,\alpha)$  reactions. The dose rates during the first week continue to be dominated by the decay of  $^{24}\text{Na}$ .  $^{54}\text{Mn}$  ( $T_{1/2} = 312.2$  d) is the dominant nuclide in the period up to ten years following shots. At times beyond 10 years after shutdown, the dose rates are

caused by the decay of the  $^{26}\text{Al}$  ( $T_{1/2} = 7.3 \times 10^5$  yr).  $^{26}\text{Al}$  is produced via the  $^{27}\text{Al}(n,2n)$  reaction.

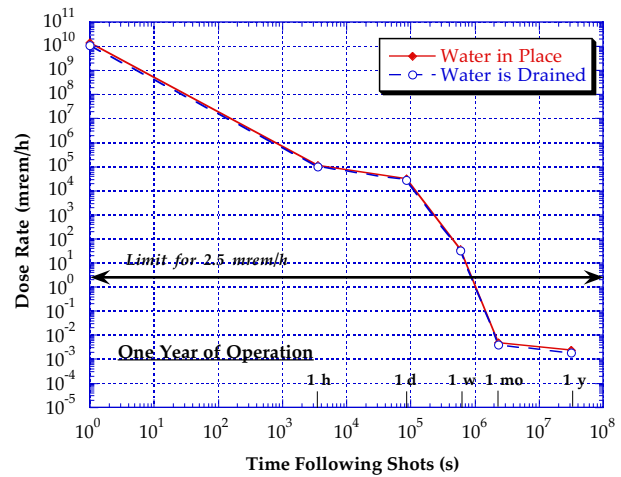


Fig. 4. Impact of Draining Water on Biological Dose Rates at Location "T1" Following Moderate Yield Shots.

In the case of the 2 1/4 Cr-1 Mo steel chamber, the dose rate during the first few minutes following shots is dominated by  $^{28}\text{Al}$  and  $^{52}\text{V}$  ( $T_{1/2} = 3.76$  min) produced from the  $^{51}\text{V}(n,\gamma)$ ,  $^{52}\text{Cr}(n,p)$ , and  $^{55}\text{Mn}(n,\alpha)$  reactions. The high content of manganese in the steel chamber results in  $^{56}\text{Mn}$  ( $T_{1/2} = 2.578$  hr) being the major contributor to the dose rate up to one day. Even though most of the  $^{56}\text{Mn}$  is produced as a result of the  $^{55}\text{Mn}(n,\gamma)$  reaction, a significant amount is also produced by the  $^{56}\text{Fe}(n,p)$  reaction. In the period between 1 day and 10 years, as in the case of the aluminum chamber,  $^{54}\text{Mn}$  and  $^{60}\text{Co}$  dominate the dose rate produced in the steel chamber. Beyond ten years after shots, the dose rate is primarily dominated by radionuclides induced from the steel impurities. The two major contributors are  $^{94}\text{Nb}$  ( $T_{1/2} = 2 \times 10^4$  yr) produced from  $^{93}\text{Nb}(n,\gamma)$  and  $^{94}\text{Mo}(n,p)$ , and  $^{93}\text{Mo}$  ( $T_{1/2} = 3,500$  yr) produced from the  $^{92}\text{Mo}(n,\gamma)$  and  $^{94}\text{Mo}(n,2n)$  reactions.

The issue of keeping water in the tank vs. draining it during maintenance as well as the possibility of using borated water instead of regular water are examined. As shown in Fig. 4, draining water from the tank will have no impact on the dose rates inside the tank (location "T1"), as in such case the dose is dominated by contribution from the chamber wall. Figure 5 shows the dose rates above the water tank (location "T2") if it is filled with either water or borated water. Replacing water in the tank with borated water did not have much of an effect on the dose rate beyond the first minute following shots. During the first minute following a shot, gammas from the decay of  $^{16}\text{N}$  ( $T_{1/2} = 7.13$  s) contribute significantly to the total dose.  $^{16}\text{N}$  is produced in water via the  $^{16}\text{O}(n,p)$  reaction. The presence of boron, with its high neutron absorption cross

section, in the borated water results in significant reduction in the amount of  $^{16}\text{N}$  generated in the tank. However, boron absorption of neutrons results in the production of a large amount of tritium. We decided that the high tritium inventory as well as the extra cost associated with the use of boron made the borated water a non-attractive alternative to water. Figure 5 also shows that the area outside the tank could be accessed following moderate shots much faster if water is kept in the tank. Keeping water in the tank helps in reducing the dose exposure from the chamber wall and reduces the dose to maintenance personnel from irradiated equipment outside the tank. In this analysis, the equipment is represented by a 50 cm thick layer of copper located a meter away from the tank surface.

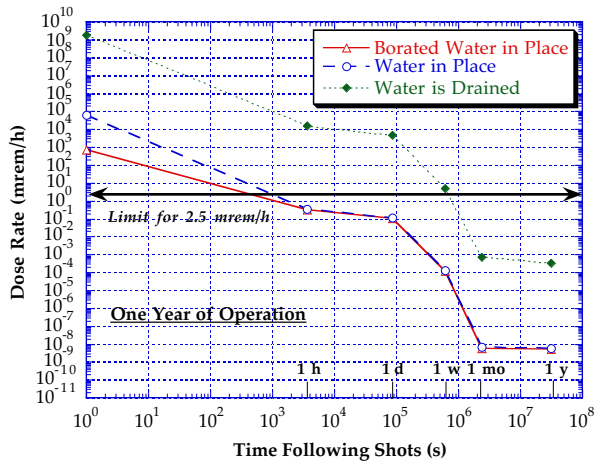


Fig. 5. Impact of Using Borated Water on Biological Dose Rates at Location "T2" Following Moderate Yield Shots.

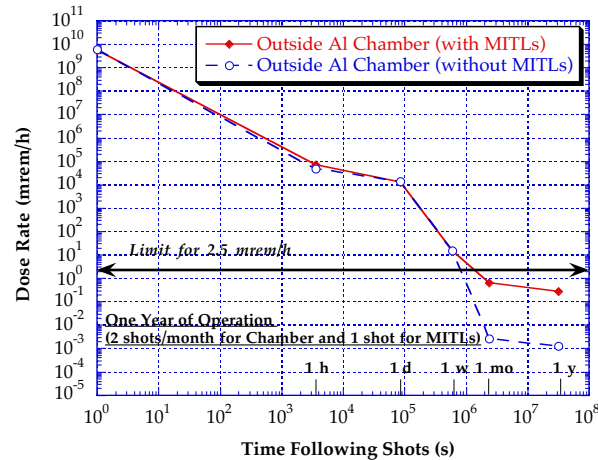


Fig. 6. Biological Dose Rates at Location "M2" Following Moderate Yield Shots.

Our analysis also showed that doses at locations at the upper side of the tank (locations "S1" and "S2") are similar to those expected at the top of the tank (locations "T1" and

"T2"). On the other hand, as shown in Fig. 6, the space in the lower part of the tank (location "M2") is better shielded during shots due to the presence of the MITLs, resulting in less activation of the chamber wall and faster access to this space following shots. However, this is only true if the force of the blast during yield shots, as expected, blows off the MITLs. The figure also shows that in the rare case where the MITLs survive the blast, a slightly higher dose is expected at location "M2" and access to this space will require a two-week waiting period. Finally, we calculated the biological dose rates inside the chamber (locations "M1") following yield shots. No hands-on maintenance could be allowed inside the chamber following moderate or high yield shots.

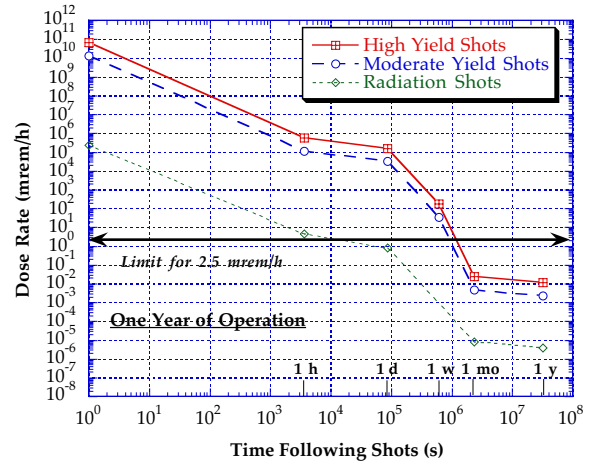


Fig. 7. Biological Dose Rates at Location "T1" Following the Three Types of Shots.

## B. Radiation Shots

During radiation shots, much smaller levels of dose are caused by the photoneutrons produced as a result of the interaction between the Bremsstrahlung radiation and the inner MITL materials. This analysis is based on total Bremsstrahlung photon production of  $5.62 \times 10^{18}$  photons per shot. The photons are assumed to be monoenergetic with a peak energy of 18 MeV. Using a conservative average iron (n,γ) cross section of 5 mb led to the production of  $9.56 \times 10^{15}$  neutrons in the inner MITLs. The neutrons have an average energy of 7 MeV. The photoneutron source is used in the neutron transport calculation to calculate the flux for activation and dose calculations. Figure 7 shows a comparison between the dose rate inside the tank following the three types of shots considered in this analysis. Dose rates outside the chamber following radiation shots are four orders of magnitude lower than dose rates following moderate yield shots. In the mean time, dose rates following high yield shots are a factor of five higher than those following moderate yield shots. As shown in Fig. 8, hands-on

maintenance activities outside the chamber may be allowed within a few hours following radiation shots. A waiting period of about a day is needed before accessing the inside of the chamber following radiation shots.

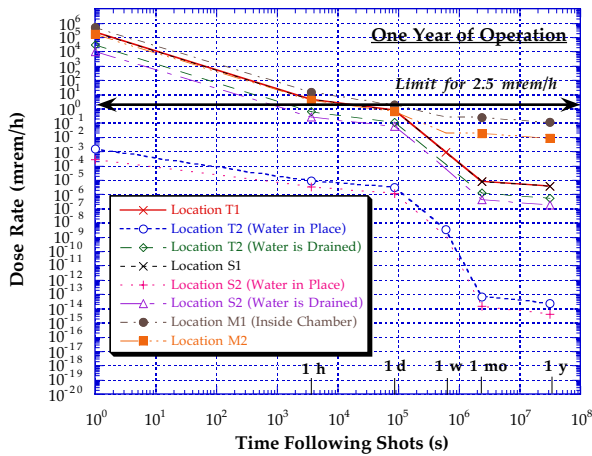


Fig. 8. Biological Dose Rates at all Locations Following Radiation Shots.

#### IV. SUMMARY

Fusion yields of up to 1000 MJ may be reached in the proposed X-1 experimental facility. The blast resulting from the explosion of the ICF fuel capsule would be confined inside an aluminum target chamber, submerged in a water tank for shielding purposes. Biological dose rates are calculated at different locations inside and outside the water tank following shots. The calculations are performed for three different types of shots. The first type is radiation shots with only photoneutrons produced during these shots. The second type of shots considered is moderate yield shots. These shots produce a fusion yield of 200 MJ. The third type of shots considered is high yield shots which generate a fusion yield of 1000 MJ. Hands-on maintenance activities outside the chamber may be allowed within a few hours following radiation shots. Dose rates outside the chamber following moderate yield shots are four orders of magnitude higher than those following radiation shots. In the mean time, dose rates following high yield shots are a factor of five higher than those following moderate yield shots. Hands-on maintenance is allowed outside the chamber and inside the water tank within 10 and 14 days following moderate and high yield shots, respectively. Access to the area outside the water filled tank is allowed after only a few hours following moderate and high yield shots.

#### ACKNOWLEDGEMENT

Support for this work was provided by Sandia National Laboratories, Albuquerque, New Mexico.

#### REFERENCES

1. G. E. Rochau et al., "Systems Analysis and Engineering of the X-1 Advanced Radiation Source," *Fusion Technology*, **34**, 825 (1998).
2. R.E. Alcouffe et al., "DANTSYS 3.0, One-, Two-, and Three-Dimensional Multigroup Discrete Ordinates Transport Code System," RSICC Computer Code Collection CCC-547, Contributed by Los Alamos National Lab, August 1995.
3. J. MacFarlane, M. Sawan, G. Moses, P. Wang, and R. Olson, "Numerical Simulation of the Explosion Dynamics and Energy Release from High-Gain ICF Targets," *Fusion Technology*, **30**, 1569 (1996).
4. J. Sisolak, et al., "DKR-PULSAR2.0: A Radioactivity Calculation Code that Includes Pulsed/Intermittent Operation," to be published.
5. A. Pashchenko et al., "FENDL/A-2.0: Neutron Activation Cross-Section Data Library for Fusion Applications," Report INDC(NDS)-173, IAEA Nuclear Data Section, March 1997.
6. H. Y. Khater and M. E. Sawan, "Dose Rate Calculations for a Light Ion Beam Fusion Laboratory Microfusion Facility," *Proceedings of the IEEE Thirteenth Symposium on Fusion Engineering*, Knoxville, TN, 1412 (1989).



## **Assessment of Personnel Accessibility in the X-1 Facility**

**H.Y. Khater, M.E. Sawan, R.R. Peterson**

**October 2000**

**UWFDM-1135**

Presented at the 14th Topical Meeting on the Technology of Fusion Energy,  
October 15–19, 2000, Park City UT

***FUSION TECHNOLOGY INSTITUTE***

***UNIVERSITY OF WISCONSIN***

***MADISON WISCONSIN***



### **DISCLAIMER**

This report was prepared as an account of work sponsored by an agency of the United States Government. Neither the United States Government, nor any agency thereof, nor any of their employees, makes any warranty, express or implied, or assumes any legal liability or responsibility for the accuracy, completeness, or usefulness of any information, apparatus, product, or process disclosed, or represents that its use would not infringe privately owned rights. Reference herein to any specific commercial product, process, or service by trade name, trademark, manufacturer, or otherwise, does not necessarily constitute or imply its endorsement, recommendation, or favoring by the United States Government or any agency thereof. The views and opinions of authors expressed herein do not necessarily state or reflect those of the United States Government or any agency thereof.

# ASSESSMENT OF PERSONNEL ACCESSIBILITY IN THE X-1 FACILITY

H. Y. Khater, M. E. Sawan and R. R. Peterson  
Fusion Technology Institute  
University of Wisconsin  
1500 Engineering Dr., Madison, WI 53706  
(608) 263-2167

## ABSTRACT

Hands-on maintenance activities outside the X-1 aluminum chamber may be allowed within a few hours following radiation (photoneutron) shots. Dose rates outside the chamber following moderate yield (200 MJ) shots are four orders of magnitude higher than those following radiation shots. In the mean time, dose rates following high yield (1000 MJ) shots are a factor of five higher than those following moderate yield shots. Hands-on maintenance is allowed outside the chamber and inside the water tank within 10 and 14 days following moderate and high yield shots, respectively. Access to the area outside the water filled tank is allowed after only a few hours following moderate and high yield shots.

## I. INTRODUCTION

The proposed X-1 experimental facility would use wire array Z-pinchs to produce X-rays for several purposes, including the radiative implosion of Inertial Confinement Fusion (ICF) capsules.<sup>1</sup> In one ICF target concept, approximately 16 MJ of X-rays would be produced by two Z-pinchs, which would be fed to a cylindrical hohlraum from both ends. The hohlraum would be designed to create the proper symmetry for the implosion for ignition of the ICF capsule. Fusion yields of up to 1000 MJ may be achievable with this approach. Another approach would place an ICF fuel capsule inside a pinch, termed a dynamic hohlraum. The blast resulting from the explosion of the capsule would be confined inside a target chamber. The fusion neutrons from yield shots and, to a lesser degree, photoneutrons and ions will activate the experimental chamber. The X-1 experiment chamber will experience a considerably harsher environment than does the National Ignition Facility (NIF) chamber. The challenge of the X-1 design activity is to develop an experiment chamber concept that allows radioactive vapor, molten material and shrapnel to be contained in a way that allows for maintenance and timely operation of the facility.

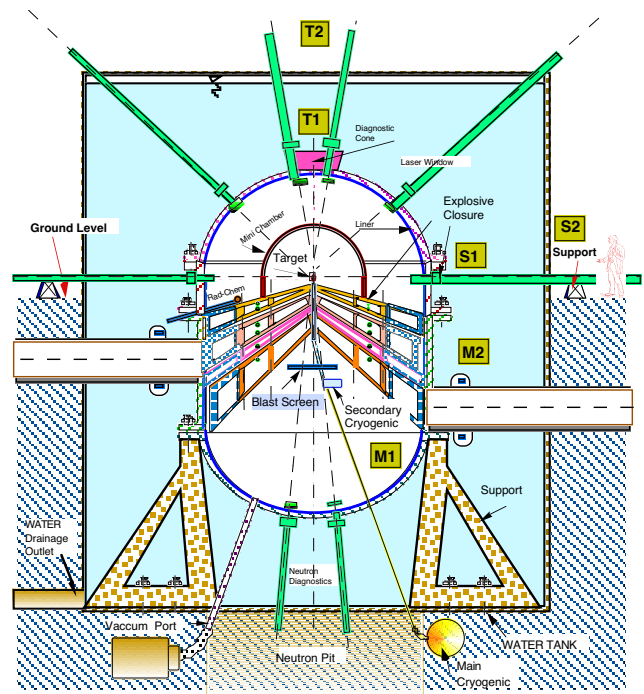


Fig. 1. X-1 Experimental Chamber Design Concept.

The experimental chamber concept is depicted in Fig. 1. The design employs a "defense in depth" strategy. Multiple layers of protection are used to confine the blast generated by the energy contained in the chamber. The first level of protection is the hemispherical mini-chamber made of Kevlar with a graphite inner coating, which is meant to stop the large pieces of magnetic debris, and most of the X-rays and debris ions emitted from the target. The mini-chamber may need replacement after shots with a burning ICF capsule, but it will be designed not to become a debris source itself. The next layer is an aluminum liner that will absorb those X-rays and debris ions that pass through the holes in the mini-chamber. Both the liner and the mini-chamber will experience

significant vaporization and melting. After a shot, the liner can be removed as a unit with the radioactive rubble trapped inside. Fast-closing explosive valves will prevent radioactive debris from leaving the experiment chamber. The liner is attached to the inner surface of an aluminum structural wall designed to carry the impulsive and long-term pressure loading from the blast. Outside of that is a water shield to stop fusion neutrons and gamma rays emitted by radioactive materials.

This experiment chamber concept is flexible with respect to its pulsed power interface. The chamber analyzed in this paper has many long coaxial magnetically insulated transmission lines (MITLs) that converge on the axis of the cylindrical chamber. In order to achieve the goal of allowing for a relatively safe maintenance environment, the blast resulting from the explosion of the ICF fuel capsule is confined inside an aluminum target chamber, submerged in a water tank for shielding purposes. In order to evaluate the radiological hazards associated with performing routine maintenance on the experimental chamber, biological dose rate calculations are performed. The dose rates are calculated at different locations in the vicinity of the chamber and following all types of shots.

## II. CALCULATION APPROACH

Neutronics and shielding calculations are performed using the ONEDANT module of the DANTSYS 3.0 discrete ordinates particle transport code system.<sup>2</sup> A spherical geometry is utilized with the target represented by an isotropic point source in the center. The source emits neutrons and gamma photons with energy spectra determined from target neutronics calculations for a generic target.<sup>3</sup> Figure 2 shows the energy spectrum of neutrons emitted from the target. The neutron flux obtained from the neutron transport calculations is used in the activation calculations. The activation calculations are performed using the computer code DKR-PULSAR<sup>4</sup> with the FENDL-2 activation cross section library.<sup>5</sup> The neutron transmutation data used is in a 46 group structure format. The gamma source data is in 21 group structure format. Using the DKR-PULSAR code allows for appropriate modeling of the pulse sequence in ICF chambers. In a previous analysis of the Laboratory Microfusion Facility,<sup>6</sup> it was shown that assuming an equivalent steady state operation (where the flux level is reduced to conserve fluence) results in underestimating the dose rates at shutdown by several orders of magnitude. The underestimation becomes negligible within a week from shutdown. The large underestimation within a short period of time following shutdown is due to the fact that the activity during this time is dominated by short-lived radionuclides. The activities of short-lived isotopes are usually sensitive to the operational schedule prior to

shutdown due to its buildup during the on time with subsequent decay during the dwell time. On the other hand, the long-term activity is dominated by long-lived radionuclides whose activity is determined by the total neutron fluence regardless of the temporal variation of the flux level.

Biological dose rates are calculated at different locations inside and outside the water tank as a function of time following shots. After initial comparison between chambers made of the Al-5083 and 2 1/4 Cr-1 Mo alloys, the low activation alloy Al-5083 is selected as the preferred chamber material candidate. The calculations are performed for three different types of shots. The first type is radiation shots with a pulsing schedule of 1 shot per day for a total of 240 shots per year. Only photoneutrons are produced during these shots. The photoneutrons are produced as a result of interaction between the Bremsstrahlung radiation and the MITLs. The second type of shots considered is moderate yield shots. These shots produce a fusion yield of 200 MJ and have a pulsing schedule of 2 shots per month for a total of 24 shots per year. The third type of shots considered is the high yield shots. These shots also use a pulsing schedule of 2 shots per month for a total of 24 shots per year with a fusion yield of 1000 MJ.

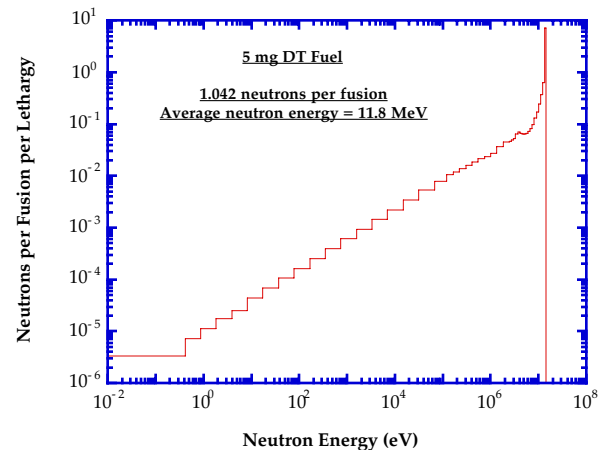


Fig. 2. Energy Spectrum of Neutrons Emitted from the Generic Target

## III. BIOLOGICAL DOSE RATES

The decay gamma source produced by the DKR-PULSAR code is used to calculate the biological dose rate after shots at different locations inside and outside the water tank. The DKR-PULSAR code gives the decay gamma source at different times following shutdown. The adjoint dose field is then determined by performing a gamma adjoint calculation using the DANTSYS code with the flux-to-dose conversion factors representing the source

at the point where the dose is calculated. The decay gamma source and the adjoint dose field are then combined to determine the biological dose rate following shutdown.

### A. Moderate and High Yield Shots

Biological dose rates are calculated at six different locations for different times following shots. These locations are shown in Fig. 1. The two alloys Al-5083 and 2 1/4 Cr-1 Mo steel are considered as chamber material candidates. Figure 3 shows a comparison between the biological dose rates expected outside the chamber and inside the water tank (location "T1") at all times following moderate yield shots for the two alloys. Using the aluminum chamber allows for hands-on maintenance, 10 days following moderate yield shots. On the other hand, using the steel chamber would not allow for hands-on maintenance at all times following shots. Based on these results, the Al-5083 alloy is selected as the preferred chamber material. The remaining results presented in this paper are for a chamber made of the Al-5083 alloy. Finally, in this analysis, the limits for hands-on maintenance were assumed to be at 2.5 mrem/hr. At these low levels, unlimited access is possible. Limited access may also be allowed at higher dose levels.

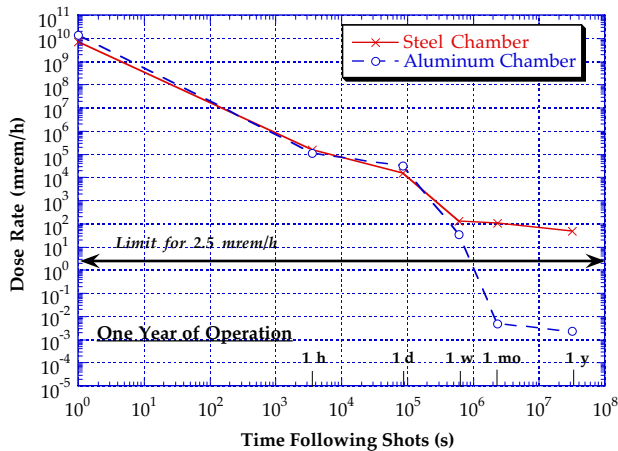


Fig. 3. Biological Dose Rates at Location "T1" Following Moderate Yield Shots.

In the case with aluminum alloy in the chamber wall, the dose rates within the first few minutes following shots are dominated by the decay of  $^{24m}\text{Na}$  ( $T_{1/2} = 20.2$  ms) produced from the  $^{27}\text{Al}(n,\alpha)$  reaction. During the first few hours, the doses are dominated by  $^{24}\text{Na}$  ( $T_{1/2} = 14.96$  hr) produced from the  $^{23}\text{Na}(n,\gamma)$ ,  $^{24}\text{Mg}(n,p)$ , and  $^{27}\text{Al}(n,\alpha)$  reactions and  $^{27}\text{Mg}$  ( $T_{1/2} = 9.45$  min) produced from the  $^{26}\text{Mg}(n,\gamma)$ ,  $^{27}\text{Al}(n,p)$ , and  $^{30}\text{Si}(n,\alpha)$  reactions. The dose rates during the first week continue to be dominated by the decay of  $^{24}\text{Na}$ .  $^{54}\text{Mn}$  ( $T_{1/2} = 312.2$  d) is the dominant nuclide in the period up to ten years following shots. At times beyond 10 years after shutdown, the dose rates are

caused by the decay of the  $^{26}\text{Al}$  ( $T_{1/2} = 7.3 \times 10^5$  yr).  $^{26}\text{Al}$  is produced via the  $^{27}\text{Al}(n,2n)$  reaction.

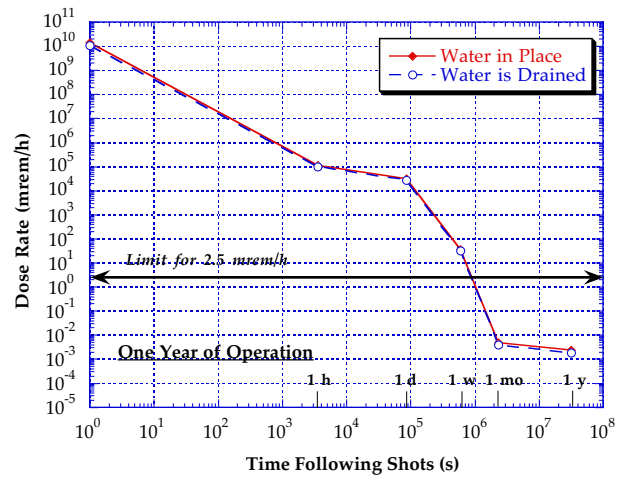


Fig. 4. Impact of Draining Water on Biological Dose Rates at Location "T1" Following Moderate Yield Shots.

In the case of the 2 1/4 Cr-1 Mo steel chamber, the dose rate during the first few minutes following shots is dominated by  $^{28}\text{Al}$  and  $^{52}\text{V}$  ( $T_{1/2} = 3.76$  min) produced from the  $^{51}\text{V}(n,\gamma)$ ,  $^{52}\text{Cr}(n,p)$ , and  $^{55}\text{Mn}(n,\alpha)$  reactions. The high content of manganese in the steel chamber results in  $^{56}\text{Mn}$  ( $T_{1/2} = 2.578$  hr) being the major contributor to the dose rate up to one day. Even though most of the  $^{56}\text{Mn}$  is produced as a result of the  $^{55}\text{Mn}(n,\gamma)$  reaction, a significant amount is also produced by the  $^{56}\text{Fe}(n,p)$  reaction. In the period between 1 day and 10 years, as in the case of the aluminum chamber,  $^{54}\text{Mn}$  and  $^{60}\text{Co}$  dominate the dose rate produced in the steel chamber. Beyond ten years after shots, the dose rate is primarily dominated by radionuclides induced from the steel impurities. The two major contributors are  $^{94}\text{Nb}$  ( $T_{1/2} = 2 \times 10^4$  yr) produced from  $^{93}\text{Nb}(n,\gamma)$  and  $^{94}\text{Mo}(n,p)$ , and  $^{93}\text{Mo}$  ( $T_{1/2} = 3,500$  yr) produced from the  $^{92}\text{Mo}(n,\gamma)$  and  $^{94}\text{Mo}(n,2n)$  reactions.

The issue of keeping water in the tank vs. draining it during maintenance as well as the possibility of using boric acid water instead of regular water are examined. As shown in Fig. 4, draining water from the tank will have no impact on the dose rates inside the tank (location "T1"), as in such case the dose is dominated by contribution from the chamber wall. Figure 5 shows the dose rates above the water tank (location "T2") if it is filled with either water or boric acid water. Replacing water in the tank with boric acid water did not have much of an effect on the dose rate beyond the first minute following shots. During the first minute following a shot, gammas from the decay of  $^{16}\text{N}$  ( $T_{1/2} = 7.13$  s) contribute significantly to the total dose.  $^{16}\text{N}$  is produced in water via the  $^{16}\text{O}(n,p)$  reaction. The presence of boron, with its high neutron absorption cross

section, in the borated water results in significant reduction in the amount of  $^{16}\text{N}$  generated in the tank. However, boron absorption of neutrons results in the production of a large amount of tritium. We decided that the high tritium inventory as well as the extra cost associated with the use of boron made the borated water a non-attractive alternative to water. Figure 5 also shows that the area outside the tank could be accessed following moderate shots much faster if water is kept in the tank. Keeping water in the tank helps in reducing the dose exposure from the chamber wall and reduces the dose to maintenance personnel from irradiated equipment outside the tank. In this analysis, the equipment is represented by a 50 cm thick layer of copper located a meter away from the tank surface.

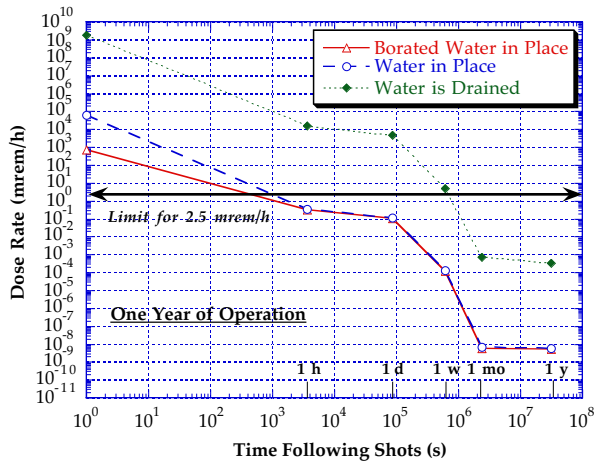


Fig. 5. Impact of Using Borated Water on Biological Dose Rates at Location "T2" Following Moderate Yield Shots.

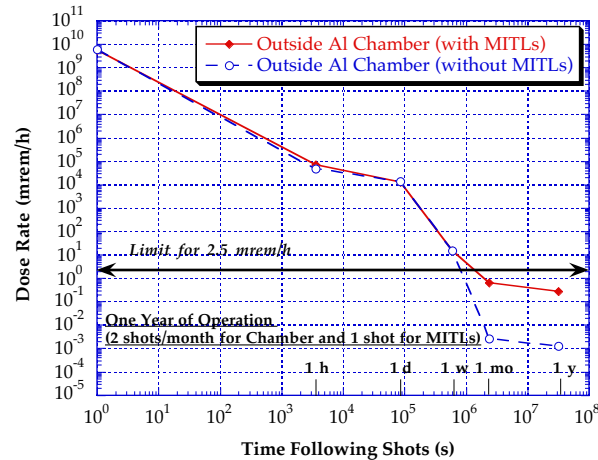


Fig. 6. Biological Dose Rates at Location "M2" Following Moderate Yield Shots.

Our analysis also showed that doses at locations at the upper side of the tank (locations "S1" and "S2") are similar to those expected at the top of the tank (locations "T1" and

"T2"). On the other hand, as shown in Fig. 6, the space in the lower part of the tank (location "M2") is better shielded during shots due to the presence of the MITLs, resulting in less activation of the chamber wall and faster access to this space following shots. However, this is only true if the force of the blast during yield shots, as expected, blows off the MITLs. The figure also shows that in the rare case where the MITLs survive the blast, a slightly higher dose is expected at location "M2" and access to this space will require a two-week waiting period. Finally, we calculated the biological dose rates inside the chamber (locations "M1") following yield shots. No hands-on maintenance could be allowed inside the chamber following moderate or high yield shots.

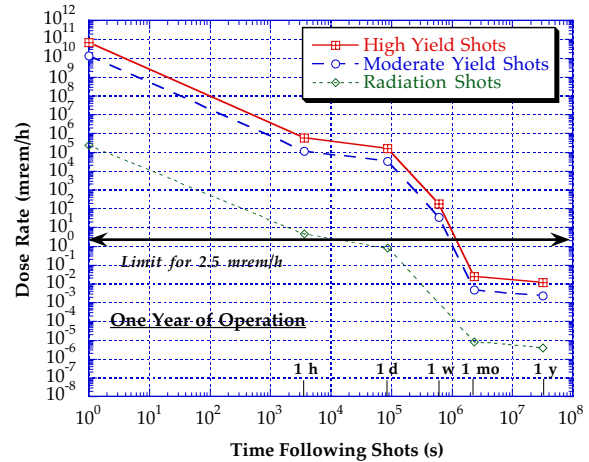


Fig. 7. Biological Dose Rates at Location "T1" Following the Three Types of Shots.

### B. Radiation Shots

During radiation shots, much smaller levels of dose are caused by the photoneutrons produced as a result of the interaction between the Bremsstrahlung radiation and the inner MITL materials. This analysis is based on total Bremsstrahlung photon production of  $5.62 \times 10^{18}$  photons per shot. The photons are assumed to be monoenergetic with a peak energy of 18 MeV. Using a conservative average iron (n,γ) cross section of 5 mb led to the production of  $9.56 \times 10^{15}$  neutrons in the inner MITLs. The neutrons have an average energy of 7 MeV. The photoneutron source is used in the neutron transport calculation to calculate the flux for activation and dose calculations. Figure 7 shows a comparison between the dose rate inside the tank following the three types of shots considered in this analysis. Dose rates outside the chamber following radiation shots are four orders of magnitude lower than dose rates following moderate yield shots. In the mean time, dose rates following high yield shots are a factor of five higher than those following moderate yield shots. As shown in Fig. 8, hands-on

maintenance activities outside the chamber may be allowed within a few hours following radiation shots. A waiting period of about a day is needed before accessing the inside of the chamber following radiation shots.

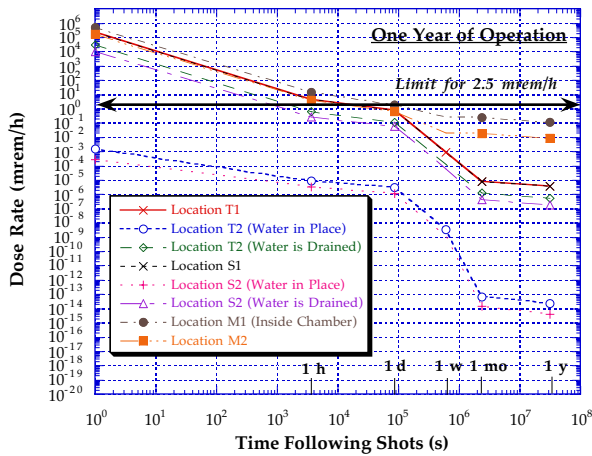


Fig. 8. Biological Dose Rates at all Locations Following Radiation Shots.

#### IV. SUMMARY

Fusion yields of up to 1000 MJ may be reached in the proposed X-1 experimental facility. The blast resulting from the explosion of the ICF fuel capsule would be confined inside an aluminum target chamber, submerged in a water tank for shielding purposes. Biological dose rates are calculated at different locations inside and outside the water tank following shots. The calculations are performed for three different types of shots. The first type is radiation shots with only photoneutrons produced during these shots. The second type of shots considered is moderate yield shots. These shots produce a fusion yield of 200 MJ. The third type of shots considered is high yield shots which generate a fusion yield of 1000 MJ. Hands-on maintenance activities outside the chamber may be allowed within a few hours following radiation shots. Dose rates outside the chamber following moderate yield shots are four orders of magnitude higher than those following radiation shots. In the mean time, dose rates following high yield shots are a factor of five higher than those following moderate yield shots. Hands-on maintenance is allowed outside the chamber and inside the water tank within 10 and 14 days following moderate and high yield shots, respectively. Access to the area outside the water filled tank is allowed after only a few hours following moderate and high yield shots.

#### ACKNOWLEDGEMENT

Support for this work was provided by Sandia National Laboratories, Albuquerque, New Mexico.

#### REFERENCES

1. G. E. Rochau et al., "Systems Analysis and Engineering of the X-1 Advanced Radiation Source," *Fusion Technology*, **34**, 825 (1998).
2. R.E. Alcouffe et al., "DANTSYS 3.0, One-, Two-, and Three-Dimensional Multigroup Discrete Ordinates Transport Code System," RSICC Computer Code Collection CCC-547, Contributed by Los Alamos National Lab, August 1995.
3. J. MacFarlane, M. Sawan, G. Moses, P. Wang, and R. Olson, "Numerical Simulation of the Explosion Dynamics and Energy Release from High-Gain ICF Targets," *Fusion Technology*, **30**, 1569 (1996).
4. J. Sisolak, et al., "DKR-PULSAR2.0: A Radioactivity Calculation Code that Includes Pulsed/Intermittent Operation," to be published.
5. A. Pashchenko et al., "FENDL/A-2.0: Neutron Activation Cross-Section Data Library for Fusion Applications," Report INDC(NDS)-173, IAEA Nuclear Data Section, March 1997.
6. H. Y. Khater and M. E. Sawan, "Dose Rate Calculations for a Light Ion Beam Fusion Laboratory Microfusion Facility," *Proceedings of the IEEE Thirteenth Symposium on Fusion Engineering*, Knoxville, TN, 1412 (1989).